Microstructure evolution at a triple junction in polycrystalline silicon

2002 J. Phys.: Condens. Matter 14 13003

(http://iopscience.iop.org/0953-8984/14/48/344)

INSTITUTE OF PHYSICS PUBLISHING JOURNAL OF PHYSICS: CONDENSED MATTER

J. Phys.: Condens. Matter **14** (2002) 13003–13008 PII: S0953-8984(02)54091-1

Microstructure evolution at a triple junction in polycrystalline silicon

Alessandra Satta[1,3], **Enrico Pisanu**[1], **Luciano Colombo**[1] **and Fabrizio Cleri**[2]

[1] INFM and Department of Physics, University of Cagliari, Cittadella Universitaria, I-09042 Monserrato (CA), Italy
[2] ENEA, Unità Materiali e Nuove Tecnologie, and INFM, CR Casaccia, CP 2400, I-00100 Roma, Italy

E-mail: alessandra.satta@dsf.unica.it

Received 27 September 2002
Published 22 November 2002
Online at stacks.iop.org/JPhysCM/14/13003

Abstract

We studied two elementary microstructure evolution events taking place at a multiple-twin triple junction (TJ) in Si by means of molecular dynamics simulations with the Stillinger–Weber empirical potential. Starting from a relaxed configuration, we inserted a fourth grain in the TJ location and determined the critical radius and the instability mode by which the central grain disappears by progressively shrinking. In a second set of simulations, we introduced a microcrack in the grain boundary plane and made it advance towards the TJ under the effect of the external loading. A kind of brittle–ductile transition is observed when the fracture changes from intergranular to intragranular.

(Some figures in this article are in colour only in the electronic version)

1. Introduction

Polycrystalline materials display a complex microstructure of grain boundaries (GBs) joining at triple junctions (TJs). GBs are the dividing surfaces (with finite thickness of a few atomic spacings) between grains with a given relative misorientation. TJs are the lines where three GBs meet. The bulk of grains may contain some density of lattice dislocations, themselves possibly arranged into a finer level of microstructure (dislocation cells, walls, etc) [1]. Over a length scale of micrometres, the evolution of polycrystalline materials can therefore be conveniently described in terms of the competition between individual extended defects, such as GBs, TJs, and dislocations. Such competition can be more clearly rationalized as an interplay among *geometrical* evolution events (e.g., GB migration and sliding, GB diffusion, plastic

[3] Author to whom any correspondence should be addressed.

deformation inside grains), which do not alter the connectivity of the GB–TJ network, and *topological* evolution events (e.g., switching between GBs, grain shrinking, grain nucleation), which can change the number and connectivity of GB–TJ network elements [2]. A similar picture can be given for the finer-scale dislocation network, its evolution being also separable into dislocation-free motion and local reactions between dislocation cores [3].

However, the interaction between extended defects takes place across widely different length scales: at the larger scale ($\sim 10^{-6}$ m) extended defects interact mainly through their elastic fields and with the externally applied fields, while at a smaller scale (i.e., when defect cores are within nanometric distance) the atomic-level structure of GBs, TJs, and dislocations determines the microstructure evolution. With respect to the above classification, it can be said that geometrical modifications are mostly dominated by the long-range elastic interaction (although the fine details of the microscopic processes, such as GB sliding, will obviously depend on the atomic structure of the GB itself), while topological modifications are dominated by the short-range (atomic) interactions.

For many purposes, the presence of lattice dislocations can be considered as a background which does not qualitatively change the picture of GBs drifting in a viscous bulk medium. This approximation provides a first simplification of the whole microstructure problem, at least over appropriate intervals of temperature, grain size, and strain or strain rate. We may thus concentrate on the competition between GBs and TJs in driving the microstructure evolution, without making any further reference to dislocations. However, the role of TJs in microstructural evolution has been the subject of debate [4–6]. Many investigators commonly attribute the evolution of grain microstructure in polycrystalline materials to GB motion only, the role of TJs thus being solely limited to equilibrating the tensions of the adjoining interfaces to ensure local equilibrium conditions. In this view, TJs do not have specific properties, such as an excess line energy or an excess volume; their properties are simply related to those of the adjoining GBs.

At variance with this scenario, recent atomistic simulations—specifically addressed to the $\Sigma 3$–$\Sigma 3$–$\Sigma 9$ multiple-twin TJ in silicon [7]—proved that such a TJ structure is indeed a true line defect, characterized by a positive excess energy of ~ 0.3 eV. This energy value was suggested to represent the upper bound to the line energy of any ordered TJ in silicon (by contrast, in random Si nanocrystals both high-energy GBs and TJs have amorphous structure [8]). It is also important to remark that the calculated excess energy of the $\Sigma 3$–$\Sigma 3$–$\Sigma 9$ TJ is of the same order as the core energy of dislocations in silicon [9]. Furthermore, a sizable volume contraction as large as $-0.29\, a_0/\omega_0$ (where $a_0 = 5.43$ Åis the Si lattice parameter at $T = 0$ K and ω_0 is the bulk atomic volume) was computed for the same $\Sigma 3$–$\Sigma 3$–$\Sigma 9$ system which, moreover, acts also as a stress concentrator with a stress field similar to that of a dislocation or a disclination [7]. On the basis of these results, we can look at TJs as elementary defects determining, in competition with GBs, microstructure evolution.

This work is aimed at elucidating some typical microstructural events that may take place at a $\Sigma 3$–$\Sigma 3$–$\Sigma 9$ TJ in Si by means of molecular dynamics simulations. Building on our previous work [7], Si is still chosen here as a model material because of its interest in the microelectronics and solar cell industry, in which the evolution of microstructural defects is a major factor controlling the electronic quality of the final material [10]. Therefore, the same Stillinger–Weber interatomic potential [11] of [7] is used to describe the directional bonding in silicon. We focus at first on the atomistic mechanism underlying the so-called T2 topological event (see, e.g., [12] and references therein), namely the mechanism by which a three-sided grain shrinks and eventually disappears from the microstructure, leaving an isolated TJ behind. We then investigate the TJ elastic and mechanical stability limit under external load and directly simulate the propagation of a microcrack in the $\Sigma 9$ GB plane, towards the TJ.

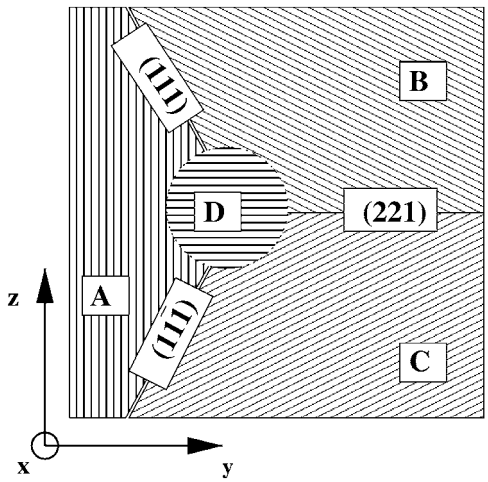

Figure 1. The geometry of the insertion of grain D at a TJ.

2. Disappearance of a three-sided grain at a triple junction

The geometry suitable for investigating the T2 event is shown in figure 1: the grain D with radius r_c is inserted at the vertex of a relaxed $\Sigma 3$–$\Sigma 3$–$\Sigma 9$ TJ, giving rise to three new TJs. In the initial TJ configuration, the crystals A/B and A/C form two non-equivalent $\{111\}\{111\}$ (or $\Sigma 3$) symmetric tilt GBs, while B/C form a $\{221\}\{221\}$ (or $\Sigma 9$) symmetric tilt GB. The grain D is chosen with such a rotation around the z-axis with respect to A, B, and C that all the surrounding interfaces correspond to high-energy GBs. Note that in this case the GB plane all around grain D is undefined, unless the relaxation is capable of lowering the surface tension (GB excess energy integrated along the interface plane) by reducing the interface to a well-defined GB. However, the initially circular shape of the inner grain D is unlikely to be fully turned into a perfectly triangular grain: in fact, the relatively small size of the simulated grains establishes a strong interface tension with the surrounding grains.

The initial radius of the inner D grain is varied in the range 2–4 a_0. The linear dimensions of the simulation cell (containing about 2×10^4 atoms) are: $L_x = \sqrt{2}\, a_0$, $L_y = 30\, a_0$, and $L_z = 60\, a_0$. With respect to the starting ideal geometry of the TJ, the insertion of the grain D sightly affects the atom density in the supercell, since it is necessary to remove no more than six atoms to accommodate the different D-grain rotations. Starting from the temperature $T = 0$ K a constant-traction molecular dynamics [13] simulation was performed to equilibrate each structure containing a given D grain up to $T = 300$ K. The system was then quenched back to $T = 0$ K. The temperature was gradually increased (or decreased) via 50 K steps and at each T-step the constant traction to the borders was accordingly adjusted.

Our main goal was to calculate the critical radius below which the three-sided inner grain becomes unstable, and to identify the mechanism through which this instability sets in. In figure 2 a snapshot of the relevant region of interest in all three samples in the final configuration is shown. The GBs relevant for the following discussion have been shaded. The instability is characterized by a progressive disordering of the inner grain D, starting from the boundary regions, when the radius is $r_c = 2\, a_0$ (see figure 2(a)): in this case the inner grain becomes like an amorphous particle and a reconstitution of the original TJ takes place. This 'amorphization path' is the microscopic mechanism by which a topological T2 (three-sided

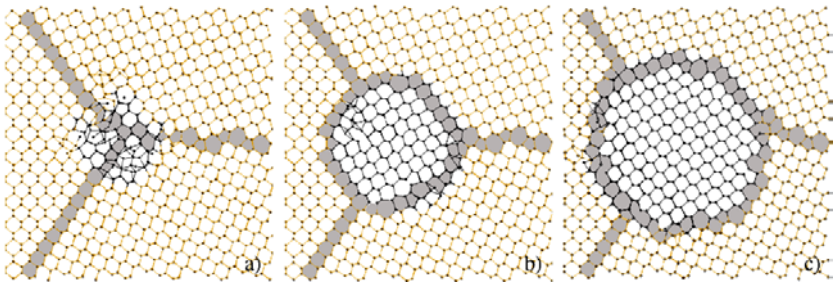

Figure 2. The final configuration for grain D after thermal annealing (see the text).

grain shrinking) event occurs in Si. It is, however, highly possible that such a mechanism is specific to Si, and that the same small-grain disappearance event in other systems (e.g., transition metals or alloys) does not necessarily involve amorphization prior to disappearance. Conversely, in the samples containing inner grains with $r_c = 3$–$4\ a_0$, as shown in figures 2(b) and (c), respectively, the inner grain is still far from the instability, its initial surface curvature being perceptibly deformed into a faceted interface. In both cases the boundary regions are mostly bulk-like except for some slight interface disorder for $r_c = 3\ a_0$, which becomes entirely negligible when $r_c = 4\ a_0$.

In order to get more detailed structural information, we calculated both the bond angle distribution function and the local atomic coordination within the (possibly) stabilized D grain. In practice, we limited our analysis to the bonding features occurring within the shaded contour shown in figure 2. Whereas for $r_c = 4\ a_0$ the bond coordination is dominantly tetrahedral, for $r_c = 2\ a_0$ a typical amorphous-like bond angle distribution is observed. This result is further confirmed by the existence of a sizable (18%) content of atoms which are not fourfold coordinated within the $r_c = 2\ a_0$ grain. The amorphization process can be attributed to an increasing interaction among the competing TJs corresponding to a decreasing size of the inner grain. When the TJ relative distance is small, a superposition of their dipolar stress fields [7] in fact occurs, locally injecting enough elastic energy to induce a crystal-to-amorphous transition.

3. Interaction between a triple junction and a propagating microcrack

GBs are usually considered a major source of degradation of the electric, thermal, and mechanical properties of polycrystalline semiconductors. In particular, GBs can represent a source of intrinsic fragility, being in general less strongly bound than bulk atomic planes. Intergranular fracture, i.e. the propagation of a crack along the GB plane between two grains, has been repeatedly investigated, from both a continuum mechanics (see, e.g., [14]) and an atomistic point of view [15, 16]. In our case, we are interested in the eventual role played by a TJ facing a crack front advancing in the GB plane.

The (non-linear) elastic effect of the external loading on the TJ is perfectly compatible with the picture of an additional elastic stress field superimposed over the elastic line tension of the TJ (disclination-like) structure. We performed a first series of simulations at $T = 0$ K to evaluate the effect of an external stress on the TJ energy and structure, again using the constant-traction MD method [13]. For relatively small values of the deformation as measured in the far field (up to $\pm 5\%$), the atomic structure of the TJ is unchanged, i.e. no plastic deformation arises as a consequence of stress relaxation. The stress map around the TJ line retains the typical dipolar, disclination-like shape.

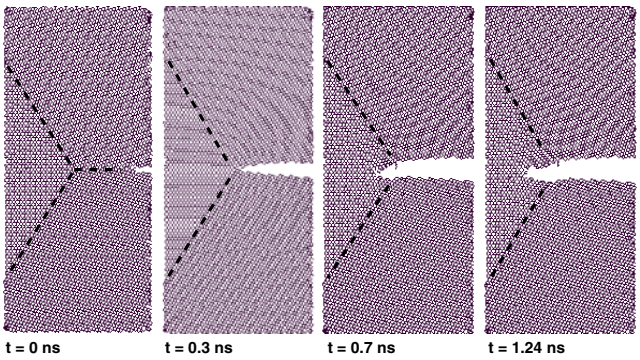

Figure 3. Crack tip propagation along the Σ9 GB and towards the Σ3–Σ3–Σ9 TJ (indicated by dashed lines).

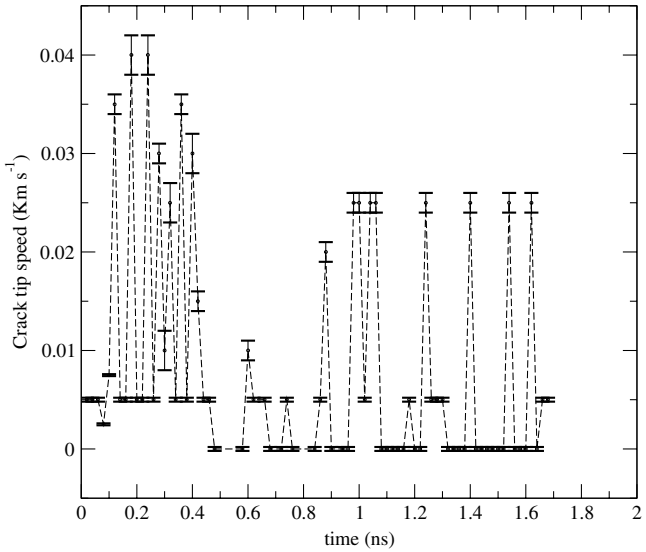

Figure 4. The crack tip propagation velocity along the Σ9 GB.

We then placed a microcrack in the Σ9 GB plane and applied an increasing load, to set the crack tip in motion towards the TJ. The sequence of snapshots in figure 3 provides a qualitative picture of the interaction between the TJ and the crack tip stress fields. The intergranular portion of crack propagation clearly has a brittle nature, the crack surfaces left behind the moving crack tip being flush with the typical steps of the vicinal $\{221\}$ surface. When the crack tip approaches the TJ it slows down, and eventually transforms into a more ductile behaviour, by breaking bonds along the $\{001\}$ plane, i.e., the bisector of the $\{111\}$ and $\{11\bar{1}\}$ GB planes. The fracture surfaces in this second portion of the crack path are much rougher, and display a clear tendency to faceting towards $\{111\}$ planes. Although no dislocations are emitted from the crack tip, the increased surface roughness and reduced crack tip speed (see below) mark a sort of brittle–ductile transition. However, the relatively small size of the simulation box in this case prevented us from further observing the steady-state propagation regime in the ductile region. Larger-scale crack propagation simulations are under way and will be presented in a forthcoming paper.

The crack tip velocity plot, reported in figure 4, clearly shows the effect of a sort of 'lattice trapping'. Note, however, that trapping as manifested in the spike character of the curve up to about $t = 0.5$ ns is not related to the breaking of individual bonds, but is rather well correlated with the successive overcoming of the vicinal steps of the adjoining $\{221\}$ surfaces in the $\Sigma 9$ GB. The 'stop-and-go' motion of the crack front should thus be related to the unlocking effect of the pseudo-dislocation cores which build up the high-angle symmetric tilt GB: when the group of bonds closest to a $\{221\}$ step is broken, a stress concentration is released and the crack tip advances briskly. In the time interval between $t = 0.5$ and 0.9 ns the crack front is almost arrested right in front of the TJ. The negative stress lobe (not shown in figure 3) locally shields the external stress field, thus reducing the local stress intensity factor K_I. This situation, which might persist indefinitely, is instead overcome when a local atomic rearrangement event breaks the TJ symmetry and allows the crack tip to resume advancing at a faster velocity—however, considerably smaller than the peak speed reached in the brittle portion of the trajectory.

Acknowledgments

This work was performed in the framework of the INFM-MUSIC and MIUR-PRIN2000 projects.

References

[1] Humphreys F J and Hatterly M 1996 *Recrystallization and Related Annealing Phenomena* (Oxford: Pergamon)
[2] Cleri F, D'Agostino G, Satta A and Colombo L 2002 *Comput. Mater. Sci.* **24** 21–7
[3] Shin C S, Fivel M C, Rodney D, Phillips R, Shenoy V B and Dupuy L 2001 *J. Physique* **11** 5–19
[4] Bollman W 1984 *Phil. Mag.* A **49** 73
Bollman W 1989 *Phil. Mag.* A **57** 637
[5] Fortier P, Palumbo G, Bruce G D, Mille W A and Aust K T 1991 *Scr. Metall. Mater.* **25** 177
[6] Srinivasan S G, Cahn J W, Jonsson H and Kalonji G 1999 *Acta Mater.* **47** 2821
[7] Costantini S, Alippi P, Colombo L and Cleri F 2001 *Phys. Rev.* B **63** 45302
[8] Keblinski P, Phillpot S R, Wolf D and Gleiter H 1997 *J. Am. Ceram. Soc.* **80** 717
[9] Bulatov V V, Yip S and Argon A 1995 *Phil. Mag.* A **72** 453
[10] Fraas L M 1978 *J. Appl. Phys.* **49** 871
[11] Stillinger F A and Weber T A 1985 *Phys. Rev.* B **31** 5262
[12] Cleri F 2000 *Physica* A **282** 339
[13] Cleri F 2001 *Phys. Rev.* B **65** 014107
[14] Beltz G E and Lipkin D M 2000 *MRS Bull.* **25** 21
[15] Cleri F, Phillpot S R and Wolf D 1999 *Interface Sci.* **7** 17
[16] Farkas D 2000 *Phil. Mag. Lett.* **80** 229